Available online at www.sciencedirect.com
SCIENCE DIRECT®
Journal of Sound and Vibration 281 (2005) 1057–1075
JOURNAL OF SOUND AND VIBRATION
www.elsevier.com/locate/jsvi

Sound radiation from forced vibration of rectangular orthotropic plates under moving loads

F.T.K. Au[a,*], M.F. Wang[b]

[a]*Department of Civil Engineering, The University of Hong Kong, Pokfulam Road, Hong Kong, People's Republic of China*
[b]*College of Civil Engineering, Hunan University, Yuelushan, Changsha, Hunan 410082, People's Republic of China*

Received 4 August 2003; received in revised form 2 January 2004; accepted 12 February 2004
Available online 25 September 2004

Abstract

This paper describes an investigation on the sound radiation from forced vibration of rectangular orthotropic plates under moving loads. The vibrations of a rectangular orthotropic thin plate with general boundary conditions traversed by moving loads are first solved. Based on the Rayleigh integral and the dynamic response of the plate, the acoustic pressure distributions around the plate are obtained in the time domain. The effects of light and heavy moving loads are separately studied. Simplified methods for calculation of the acoustic pressure distributions in far field are developed. The effects of moving mass, damping coefficient, boundary conditions and moving speed on the dynamic responses of the plate and the acoustic pressure distributions are investigated.

1. Introduction

Many researchers have studied the vibrations of plates and the sound radiation from them because of its importance in engineering. Extensive research on the vibration and acoustic responses of a plate subjected to a stationary harmonic point load has been done in the past. The corresponding case with moving loads is probably of more practical interest to civil engineers. Many types of bridges, such as solid or voided slab decks and beam-and-slab decks, can be

*Corresponding author. Tel.: +852-2859-2650; fax: +852-2559-5337.
E-mail address: francis.au@hku.hk (F.T.K. Au).

0022-460X/$ - see front matter © 2004 Elsevier Ltd. All rights reserved.
doi:10.1016/j.jsv.2004.02.005

modelled as orthotropic plates with two different moduli. The evaluation of structure-borne noise of a highway or railway bridge can be considered as an orthotropic plate with moving loads. However, little work on this area has been done probably because of the difficulty and the plethora of factors and uncertainties involved.

The dynamic response of isotropic plates under moving loads has been well studied, and classical solutions have been obtained by Raske and Schlack [1] and Fryba [2]. Using the finite element method, Yoshida and Weaver [3] and Wu et al. [4] analysed the dynamic responses of plates subjected to various types of moving loads. Gbadeyan and Oni [5] presented some analytical results for the dynamic behaviour of rectangular plates under moving loads based on modified generalized finite integral transforms and the modified Struble's method. By modelling the rectangular bridge deck by orthotropic plate elements and the vehicle as a single sprung mass moving along the deck, Humar and Kashif [6] solved the vehicle–bridge interaction problem and identified the parameters governing the dynamic response. Takabatake [7] presented a simplified analytical method for rectangular plates with stepped thickness subjected to moving loads using a characteristic function to account for the discontinuous variation of the bending stiffness and mass of the plate. The effect of the additional mass due to moving loads was also examined. Using the large deflection theory of the Mindlin plate and Galerkin's method, Wang and Kuo [8] examined the static responses of a plate produced by its own weight and its dynamic responses caused by the coupling effect of these static responses with a set of moving forces. To obtain the vibration of a slab bridge subjected to a convoy of moving vehicles, Cheung et al. [9] presented a numerical method that combined the benefits offered by the structural impedance method and finite strip method so that the bridge and the vehicles could be separately considered with their interaction dealt with subsequently. Shadnam et al. [10] investigated the dynamics of plates under the influence of relatively large moving masses and concluded that the response of structures due to moving mass must be properly taken into account.

A lot of work has been done on the estimation of sound radiation from vibrating plates. Maidanik [11] investigated the single-mode radiation resistance of a finite, simply supported baffled plate. Wallace [12] carried out a theoretical study on a finite rectangular panel by considering the energy radiated by a mode of the panel into the far field. The method yielded low-frequency asymptotic solutions and permitted a precise numerical determination of the radiation resistance over the entire frequency range. Maidanik [13] gave an asymptotic formula for the radiation coefficients, which is still widely used. Williams and Maynard [14] suggested a numerical method for evaluation of the Rayleigh integral for planar radiators using the FFT. Schedin et al. [15] reported a comparison between measured and simulated transient acoustic fields generated by a thin rectangular impacted steel plate. The plate vibration was modelled in the time domain using a finite difference scheme while the radiated acoustic was obtained by solving numerically the Rayleigh integral equation by a simple boundary element method. The state of the art has been summarized by Fahy [16] and Cremer et al. [17].

This paper describes an investigation on the sound radiation from forced vibration of rectangular orthotropic plates with general boundary conditions under moving loads. Apart from the development of efficient computational methods for evaluation of the structure-borne noise, the cases that give rise to high vibration and sound radiation levels are identified. After solving for the forced vibration of the plates for different cases, this paper presents some theoretical predictions of the radiation acoustic field of the plate together with some simplified methods to

obtain the acoustic pressure distributions in far field. The effects of the mass ratios, speed and boundary conditions on the radiation acoustic field are studied.

2. Rectangular orthotropic plates under moving loads

2.1. Governing equations and general solution

A moving load F_p is moving at speed v_x on a rectangular orthotropic plate of length a and breadth b as shown in Fig. 1. The inertia effect of the moving load may or may not be considered depending on the mass involved. The equation of motion and the initial conditions can be written as

$$D_x\frac{\partial^4 w}{\partial x^4}+2H\frac{\partial^4 w}{\partial x^2\partial y^2}+D_y\frac{\partial^4 w}{\partial y^4}+c_d\frac{\partial w}{\partial t}+\rho h\frac{\partial^2 w}{\partial t^2}=p(x,y,t)\delta(x-\upsilon_x t)\delta(y-e_0-\upsilon_y t), \tag{1}$$

$$w(x,y,t)|_{t=0}=w(x,y,0),\quad \dot{w}(x,y,t)|_{t=0}=\dot{w}(x,y,0), \tag{2}$$

where D_x and D_y are the flexural rigidities in the x and y directions respectively, D_{xy} is the torsional rigidity, H is the equivalent rigidity taken as $v_yD_x+2D_{xy}$ or $v_xD_y+2D_{xy}$, h is the thickness of the plate, ρ is the mass density of plate, v_x and v_y are Poisson's ratios in the x and y directions, respectively, and c_d is the damping coefficient of the plate. Note that the moving load is expressed in terms of the magnitude $p(x,y,t)$ of the load, the velocity components υ_x and υ_y in the x and y directions, the Dirac Delta functions $\delta(x)$ and $\delta(y)$ to define the coordinates of the loaded point, and the distance e_0 between the path and the x-axis. The displacement $w(x,y,t)$ at point (x,y) of the plate at time t can be written by modal superposition as

$$w(x,y,t)=\sum_{m=1}^{\infty}\sum_{n=1}^{\infty}U_{mn}(x,y)q_{mn}(t), \tag{3}$$

where $U_{mn}(x,y)$ is a typical mode shape with associated natural frequency ω_{mn} of the plate that can be obtained using the methods by Huffington and Hoppmann [18] or Leissa [19], and $q_{mn}(t)$ is the corresponding modal coordinate. Note that the mode shapes and associated natural frequencies used for subsequent analysis are those of the plate taking no account of the inertia

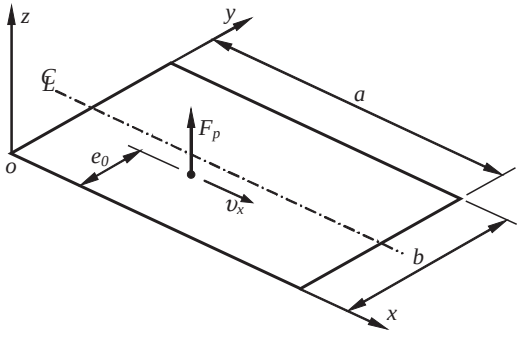

Fig. 1. A rectangular orthotropic plate under a moving load.

effect of the moving load. Substituting Eq. (3) into Eq. (1) results in the decoupled equations in terms of the modal coordinates. Using the modal orthogonality conditions and assuming proportional damping in the system give the normalised equation of motion

$$\ddot{q}_{mn}(t) + 2\zeta_{mn}\omega_{mn}\dot{q}_{mn}(t) + \omega_{mn}^2 q_{mn}(t) = p_{mn}(t), \tag{4}$$

where the generalised mass of the plate $\tilde{m}_{mn}$, the generalised damping factor ζ_{mn}, the generalised natural frequency ω_{mn} and the normalised force $p_{mn}(t)$ are given, respectively, by

$$\tilde{m}_{mn} = \int_0^a \int_0^b \rho h U_{mn}^2(x,y)\,\mathrm{d}x\,\mathrm{d}y, \tag{5}$$

$$\zeta_{mn} = c_d/2\rho h\omega_{mn}, \tag{6}$$

$$\omega_{mn}^2 = \frac{1}{\tilde{m}_{mn}} \int_0^a \int_0^b \left(D_x \frac{\partial^4 U_{mn}}{\partial x^4} + 2H \frac{\partial^4 U_{mn}}{\partial x^2 \partial y^2} + D_y \frac{\partial^4 U_{mn}}{\partial y^4} \right) U_{mn}\,\mathrm{d}x\,\mathrm{d}y, \tag{7}$$

$$p_{mn}(t) = p(\upsilon_x t, y_0 + \upsilon_y t, t) U_{mn}(\upsilon_x t, e_0 + \upsilon_y t)/\tilde{m}_{mn}. \tag{8}$$

For a lightly damped system (i.e. $\zeta_{mn} < 1.0$), Eq. (4) can be solved in the time domain by Duhamel integral, giving the generalised displacement $q_{mn}(t)$ as

$$\begin{aligned} q_{mn}(t) = {} & \exp(-\zeta_{mn}\omega_{mn}t)(a_{mn} \sin \varpi_{mn}t + b_{mn} \cos \varpi_{mn}t) \\ & + \frac{1}{\varpi_{mn}} \int_0^t p_{mn}(\tau) \exp(-\zeta_{mn}\omega_{mn}(t-\tau)) \sin \varpi_{mn}(t-\tau)\,\mathrm{d}\tau, \end{aligned} \tag{9}$$

where the generalised natural frequency of damped free vibration ϖ_{mn} is defined as

$$\varpi_{mn} = \omega_{mn}\sqrt{1-\zeta_{mn}^2} \tag{10}$$

and the parameters a_{mn} and b_{mn} can be determined from the initial conditions $w(x,y,0)$ and $\dot{w}(x,y,0)$ shown in Eq. (2) as

$$a_{mn} = \frac{\int_0^a \int_0^b (\dot{w}(x,y,0) + 2\zeta_{mn}\omega_{mn} w(x,y,0)) U_{mn}\,\mathrm{d}x\,\mathrm{d}y}{\varpi_{mn} \int_0^a \int_0^b U_{mn}^2\,\mathrm{d}x\,\mathrm{d}y}, \tag{11}$$

$$b_{mn} = \frac{\int_0^a \int_0^b w(x,y,0) U_{mn}\,\mathrm{d}x\,\mathrm{d}y}{\int_0^a \int_0^b U_{mn}^2 \mathrm{d}x\,\mathrm{d}y}. \tag{12}$$

The dynamic responses of the plate may be divided into three different stages, including the initial free vibration, the forced vibration under the moving load and the free vibration after the moving load has left. The initial free vibration compatible with the initial conditions $w(x,y,0)$ and $\dot{w}(x,y,0)$ described by Eq. (2) is simply the first part of Eq. (9). After the moving load leaves the plate at time t_k, the ensuing free vibration can be similarly determined in terms of the conditions $w(x,y,t_k)$ and $\dot{w}(x,y,t_k)$ then. Differentiation of Eq. (9) gives the generalised velocity $\dot{q}_{mn}(t)$ while the generalised acceleration $\ddot{q}_{mn}(t)$ can be obtained by substituting $q_{mn}(t)$ and $\dot{q}_{mn}(t)$ into Eq. (4). Substituting the generalised displacement $q_{mn}(t)$ from Eq. (9) into Eq. (3) gives the displacement $w(x,y,t)$ of the plate at point (x, y) and time t. The velocity $\dot{w}(x,y,t)$ and acceleration $\ddot{w}(x,y,t)$ of

the plate can be worked out by differentiation. If there are multiple moving loads, the above procedures can still be applied with the help of superposition.

2.2. Plates with different boundary conditions

Various methods are available to deal with rectangular plates with different boundary conditions. Rectangular plates having one or two pairs of opposite simply supported edges allow more straightforward analysis. The typical mode shape $U_{mn}(x,y)$ of a rectangular plate with at least a pair of opposite simply supported edges [18] at $x=0$ and $x=a$ can be written in terms of the parameter $\lambda_m = m\pi/a$ as

$$U_{mn}(x,y) = Y_{mn}(y)\,\sin\,\lambda_m x, \tag{13}$$

where the transverse shape function $Y_{mn}(y)$ is expressed in terms of the parameters ϕ_{mn} and ψ_{mn}, and the constants C_{imn} that can be determined from the boundary conditions as

$$Y_{mn}(y) = C_{1mn}\,\mathrm{ch}\left(\frac{\phi_{mn}y}{a}\right) + C_{2mn}\,\mathrm{sh}\left(\frac{\phi_{mn}y}{a}\right) + C_{3mn}\,\cos\left(\frac{\psi_{mn}y}{a}\right) + C_{4mn}\,\sin\left(\frac{\psi_{mn}y}{a}\right). \tag{14}$$

The parameters ϕ_{mn} and ψ_{mn} to build up the transverse displacement function $Y_{mn}(y)$ are given explicitly as

$$\phi_{mn} = \frac{m\pi}{\sqrt{D_y}}\sqrt{\sqrt{\left(H^2 - D_xD_y + \frac{\rho h D_y a^4\omega_{mn}^2}{m^4\pi^4}\right)} + H}, \tag{15}$$

$$\psi_{mn} = \frac{m\pi}{\sqrt{D_y}}\sqrt{\sqrt{\left(H^2 - D_xD_y + \frac{\rho h D_y a^4\omega_{mn}^2}{m^4\pi^4}\right)} - H} \tag{16}$$

in terms of the circular frequency

$$\omega_{mn} = \frac{1}{a^2\sqrt{\rho h}}\sqrt{D_y\phi_{mn}^4 - 2m^2\pi^2 H\phi_{mn}^2 + m^4\pi^4 D_x}. \tag{17}$$

Note that the parameters ϕ_{mn} and ψ_{mn} are not independent but are related by

$$\phi_{mn}^2 - \psi_{mn}^2 = 2m^2\pi^2 H/D_y. \tag{18}$$

For rectangular plates simply supported on all the four sides, the transverse shape function $Y_{mn}(y)$ and circular frequency ω_{mn} [18] are given in terms of the parameter $\mu_n = n\pi/b$ as

$$Y_{mn}(y) = \sin\,\mu_n y, \tag{19}$$

$$\omega_{mn} = \frac{1}{\sqrt{\rho h}}\sqrt{\lambda_m^4 D_x + 2\lambda_m^2\mu_n^2 H + \mu_n^4 D_y}. \tag{20}$$

For rectangular plates simply supported at $x=0$ and $x=a$ with the two other sides free, the frequency equation of the plate [18] is

$$(\psi_{mn}^2\gamma_{mn}^4 - \phi_{mn}^2\delta_{mn}^4)\mathrm{sh}\,\phi_{mn}r\,\sin\,\psi_{mn}r + 2\phi_{mn}\psi_{mn}\gamma_{mn}^2\delta_{mn}^2(\mathrm{ch}\,\phi_{mn}r\,\cos\,\psi_{mn}r - 1) = 0, \tag{21}$$

where

$$\gamma_{mn} = (\phi_{mn}^2 - m^2\pi^2 v_x)D_y, \quad \delta_{mn} = (\psi_{mn}^2 + m^2\pi^2 v_x)D_y, \quad r = b/a. \tag{22-24}$$

The constants C_{imn} of the transverse shape function $Y_{mn}(y)$ in Eq. (14) are

$$C_{1mn} = \delta_{mn}/[\gamma_{mn}\delta_{mn}(\mathrm{ch}\,\phi_{mn}r - \cos\,\psi_{mn}r)], \tag{25}$$

$$C_{2mn} = -\psi_{mn}\gamma_{mn}/(\psi_{mn}\gamma_{mn}^2\,\mathrm{sh}\,\phi_{mn}r - \phi_{mn}\delta_{mn}^2\,\sin\,\psi_{mn}r), \tag{26}$$

$$C_{3mn} = \gamma_{mn}/[\gamma_{mn}\delta_{mn}(\mathrm{ch}\,\phi_{mn}r - \cos\,\psi_{mn}r)], \tag{27}$$

$$C_{4mn} = -\phi_{mn}\delta_{mn}/(\psi_{mn}\gamma_{mn}^2\,\mathrm{sh}\,\phi_{mn}r - \phi_{mn}\delta_{mn}^2\,\sin\,\psi_{mn}r). \tag{28}$$

The parameters ϕ_{mn} and ψ_{mn} can be solved from Eqs. (18) and (21), while the circular frequency ω_{mn} can be obtained from Eq. (17).

For rectangular plates not having a pair of opposite simply supported sides, the typical mode shape $U_{mn}(x, y)$ [19] can be written as

$$U_{mn}(x, y) = X_m(x)\,Y_n(y), \tag{29}$$

where $X_m(x)$ and $Y_n(y)$ are taken to be the mode shapes of the associated undamped beams having the same boundary conditions as the plate in the x and y directions, respectively, which are of the form

$$X_m(x) = A_{1m}\,\sin\,\alpha_m x + A_{2m}\,\cos\,\alpha_m x + A_{3m}\,\mathrm{sh}\,\alpha_m x + A_{4m}\,\mathrm{ch}\,\alpha_m x, \tag{30}$$

$$Y_n(y) = B_{1n}\,\sin\,\beta_n y + B_{2n}\,\cos\,\beta_n y + B_{3n}\,\mathrm{sh}\,\beta_n y + B_{4n}\,\mathrm{ch}\,\beta_n y. \tag{31}$$

Substituting Eq. (29) into Eq. (7), the circular frequency ω_{mn} is obtained as

$$\omega_{mn}^2 = \frac{1}{\tilde{m}_{mn}}\int_0^a\int_0^b [(D_x\alpha_m^4 + D_y\beta_n^4)X_m^2(x)\,Y_n^2(y) + 2HX_m(x)\,Y_n(y)\,Y_m''(x)\,Y_n''(y)]\,\mathrm{d}x\,\mathrm{d}y. \tag{32}$$

For a rectangular plate clamped on four sides, the parameters in Eqs. (30) and (31) are

$$A_{1m} = -A_{3m} = 1, \quad A_{2m} = -A_{4m} = \frac{\mathrm{sh}\,\alpha_m a - \sin\,\alpha_m a}{\cos\,\alpha_m a - \mathrm{ch}\,\alpha_m a}, \tag{33}$$

$$B_{1n} = -B_{3n} = 1, \quad B_{2n} = -B_{4n} = \frac{\mathrm{sh}\,\beta_m b - \sin\,\beta_m b}{\cos\,\beta_m b - \mathrm{ch}\,\beta_m b}, \tag{34}$$

$$\alpha_m = \lambda_m/a, \;\; \beta_n = \lambda_n/b \quad (m = 1, 2, \ldots;\; n = 1, 2, \ldots), \tag{35}$$

where the parameters λ_m and λ_n in the two directions can be obtained from the same equation for a clamped beam

$$\mathrm{ch}\,\lambda\,\cos\,\lambda - 1 = 0. \tag{36}$$

Substituting Eqs. (33)–(36) into Eq. (32), the circular frequency ω_{mn} can be obtained.

2.3. Solution strategy

Consider the case of a constant load p_0 moving at a constant speed v_x in the x-direction (i.e. $v_y = 0$) at a distance e_0 from the x-axis. The actual force $p(x, y, t)$ may be written in terms of the mass of the moving load $\mu_p = p_0/g$ as

$$p(x, y, t) = p_0 - \mu_p \left(\frac{\partial^2 w}{\partial x^2} v_x^2 + 2 \frac{\partial^2 w}{\partial x \, \partial t} v_x + \frac{\partial^2 w}{\partial t^2} \right), \tag{37}$$

where g is the acceleration due to gravity. Let the mass ratio be the ratio of the mass of the moving load to that of the plate. For a low mass ratio, the inertia effect of the moving load can be neglected and therefore the mass μ_p in Eq. (37) can be taken as zero. Further simplification is possible as $p(x, y, t) = p_0$. If the initial free vibration is neglected, substituting the resulting normalised force $p_{mn}(t)$ from Eq. (8) into Eqs. (9) and (3), the displacement of the plate under the forced vibration of the moving load can be obtained as

$$w(x, y, t) = \sum_{m=1}^{\infty} \sum_{n=1}^{\infty} \frac{p_0 U_{mn}(x, y)}{\varpi_{mn} \tilde{m}_{mn}} \int_0^t \exp(-\zeta_{mn} \omega_{mn} (t - \tau)) U_{mn}(v_x \tau, e_0) \sin(\varpi_{mn} (t - \tau)) \, \mathrm{d}\tau. \tag{38}$$

The velocity $\dot{w}(x, y, t)$ and the acceleration $\ddot{w}(x, y, t)$ of the plate can therefore be obtained by differentiation.

However, when the mass ratio is high, the inertia effect of moving load cannot be neglected. Substituting Eqs. (37) and (3) into Eq. (1) results in equations in terms of the modal coordinates. The normalised equation of motion can be obtained by using the modal orthogonality conditions and assuming proportional damping in the system as

$$\ddot{q}_{mn}(t) + 2\zeta_{mn} \omega_{mn} \dot{q}_{mn}(t) + \omega_{mn}^2 q_{mn}(t) = p_{mn}^*(t), \tag{39}$$

where the normalised force $p_{mn}^*(t)$ has the modified form

$$p_{mn}^*(t) = p_{mn}(t) - \frac{\mu_p U_{mn}}{\tilde{m}_{mn}} \sum_{m=1}^{\infty} \sum_{n=1}^{\infty} \left(v_x^2 \frac{\partial^2 U_{mn}}{\partial x^2} q_{mn}(t) + 2 v_x \frac{\partial U_{mn}}{\partial x} \dot{q}_{mn}(t) + U_{mn} \ddot{q}_{mn}(t) \right) \Bigg|_{\substack{x = v_x t \\ y = e_0}}. \tag{40}$$

It should be pointed out that Eq. (39) is indeed coupled because of the normalised force $p_{mn}^*(t)$ on the right-hand side. If the m and n indices in Eq. (39) are truncated after m_u and n_u terms, respectively, it can be written in matrix form as

$$([I] + [M_m])\{\ddot{Q}\} + ([C_d] + [C_m])\{\dot{Q}\} + ([K_d] + [K_m])\{Q\} = \{P\}, \tag{41}$$

where $[I]$ is the identity matrix that results from normalisation by the generalised mass of the plate $\tilde{m}_{mn}$, and the modal coordinates $q_{mn}(t)$ are arranged in the vector $\{Q\}$ as

$$\{Q\} = [q_{11} \cdots q_{1n_u} \cdots q_{m_u 1} \cdots q_{m_u n_u}]^{\mathrm{T}} \tag{42}$$

and the velocity vector $\{\dot{Q}\}$ and acceleration vector $\{\ddot{Q}\}$ are similarly the first and second derivatives of $\{Q\}$ with respect to time t. The explicit forms of the generalised mass matrix $[M_m]$ to reflect the inertia effect of the moving load, the generalised damping matrices $[C_d]$ and $[C_m]$, the generalised stiffness matrices $[K_d]$ and $[K_m]$, and the generalised load vector $\{P\}$ are given in Appendix A.1. The modal responses $\{Q\}$, $\{\dot{Q}\}$ and $\{\ddot{Q}\}$ in Eq. (41) can be solved by a suitable

higher-order numerical integration method [20]. Thereafter, the dynamic responses of the plate can be obtained by substituting $\{Q\}$, $\{\dot{Q}\}$ and $\{\ddot{Q}\}$ into Eq. (3).

3. Calculation of acoustic pressure distribution

3.1. General formulae for acoustic pressure distribution

The acoustic pressure radiated from a vibration plate in an infinite baffle can be obtained by evaluating the Rayleigh surface integral where each elemental area on the plate surface is regarded as a simple point source of an outgoing wave and its contribution is added with an appropriate time delay. Referring to Fig. 2, the acoustic pressure $F_{\text{pres}}(x_0, y_0, z_0, t)$ at the observation point P with Cartesian coordinates (x_0, y_0, z_0) at time t caused by the vibration of the plate is given by

$$F_{\text{pres}}(x_0, y_0, z_0, t) = \frac{\rho_0}{2\pi} \int_0^a \int_0^b \ddot{w}\left(x, y, t - \frac{R}{c}\right) \frac{1}{R} \, \mathrm{d}x \, \mathrm{d}y \tag{43}$$

where ρ_0 and c are, respectively, the mass density and wave velocity of the acoustic medium, $\ddot{w}(x, y, t)$ is the acceleration time history of the plate obtained previously, and R is the distance between the observation point P and the infinitesimal element at (x, y) on the plate surface. The observation point P can alternatively be described by its spherical coordinates (r, θ, ϕ) as shown in Fig. 2, where r is the distance from the observation point P to the origin. The near and far acoustic fields of the plate are then analysed according to Eq. (43).

Using the standard trapezoidal rule [15] in which the side a is divided into N_x equal segments Δx (i.e. $a = N_x \Delta x$) and the side b is divided into N_y equal segments Δy (i.e. $b = N_y \Delta y$), the acoustic pressure for rectangular plates under a light moving load can be computed from

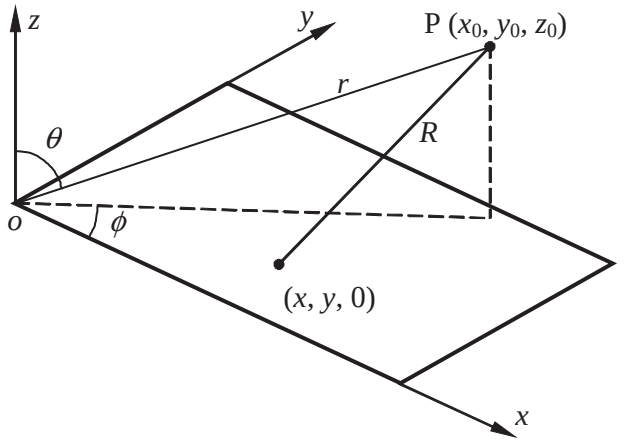

Fig. 2. Coordinate system used for evaluation of acoustic pressure.

Eq. (43) as

$$F_{\text{pres}}(x_0,y_0,z_0,t)=\frac{\rho_0\Delta x\Delta y}{8\pi}\sum_{i=0}^{N_x-1}\sum_{j=0}^{N_y-1}\left\{\frac{\ddot{w}(i\Delta x,j\Delta y,t-R_{i,j}/c)}{R_{i,j}}+\frac{\ddot{w}((i+1)\Delta x,j\Delta y,t-R_{i+1,j}/c)}{R_{i+1,j}}\right.$$
$$\left.+\frac{\ddot{w}(i\Delta x,(j+1)\Delta y,t-R_{i,j+1}/c)}{R_{i,j+1}}+\frac{\ddot{w}((i+1)\Delta x,(j+1)\Delta y,t-R_{i+1,j+1}/c)}{R_{i+1,j+1}}\right\}, \tag{44}$$

where the distance $R_{i,j}$ between the observation point P and the grid point at coordinates $(i\Delta x, j\Delta y)$ on the plate is given by

$$R_{i,j}=\sqrt{(x_0-i\Delta x)^2+(y_0-j\Delta y)^2+z_0^2}. \tag{45}$$

The corresponding formula for rectangular plates under heavy moving loads can be obtained by substituting the solution to Eq. (41) into Eq. (43), giving

$$F_{\text{pres}}(x_0,y_0,z_0,t)=\frac{\rho_0\Delta x\Delta y}{8\pi}\sum_{i=0}^{N_x-1}\sum_{j=0}^{N_y-1}\sum_{m=1}^{\infty}\sum_{n=1}^{\infty}\left\{\frac{U_{mn}(i\Delta x,j\Delta y)}{R_{i,j}}\ddot{q}_{mn}\left(t-\frac{R_{i,j}}{c}\right)\right.$$
$$+\frac{U_{mn}((i+1)\Delta x,j\Delta y)}{R_{i+1,j}}\ddot{q}_{mn}\left(t-\frac{R_{i+1,j}}{c}\right)+\frac{U_{mn}(i\Delta x,(j+1)\Delta y)}{R_{i,j+1}}\ddot{q}_{mn}\left(t-\frac{R_{i,j+1}}{c}\right)$$
$$\left.+\frac{U_{mn}((i+1)\Delta x,(j+1)\Delta y)}{R_{i+1,j+1}}\ddot{q}_{mn}\left(t-\frac{R_{i+1,j+1}}{c}\right)\right\}. \tag{46}$$

3.2. Acoustic pressure distribution in the far field of plates under light moving loads

In the far field of the plate (i.e. $r\gg a,b$), Eq. (43) can be further simplified for the case of light moving loads. With reference to Fig. 2, the distance R can be approximated by

$$R\approx r-\frac{x_0}{r}x-\frac{y_0}{r}y=r-x\sin\theta\cos\phi-y\sin\theta\sin\phi. \tag{47}$$

When the damping effect is negligible (i.e. $\zeta_{mn}=0$), the acoustic pressure caused by a rectangular orthotropic plate with general boundary conditions by a light moving load may be estimated by

$$F_{\text{pres}}(x_0,y_0,z_0,t)=\frac{\rho_0 p_0}{2\pi r}\sum_{m=1}^{\infty}\sum_{n=1}^{\infty}\frac{Y_n(e_0)}{\tilde{m}_{mn}}\{\Delta_{1mn}(a_{12}^{mn}a_{22}^{mn}-a_{11}^{mn}a_{21}^{mn})+\Delta_{2mn}(a_{11}^{mn}a_{22}^{mn}+a_{12}^{mn}a_{21}^{mn})$$
$$+\Delta_{3mn}(b_{12}^{mn}b_{22}^{mn}-b_{11}^{mn}b_{21}^{mn})+\Delta_{4mn}(b_{11}^{mn}b_{22}^{mn}+b_{12}^{mn}b_{21}^{mn})+\Delta_{5mn}(c_{12}^{mn}c_{22}^{mn}+c_{11}^{mn}c_{21}^{mn})$$
$$+\Delta_{6mn}(c_{11}^{mn}c_{22}^{mn}+c_{12}^{mn}c_{21}^{mn})\} \tag{48}$$

where the parameters $\Delta_{1mn}-\Delta_{6mn}$, and a_{ij}^{mn}, b_{ij}^{mn} and c_{ij}^{mn} $(i,j=1,2)$ are given in Appendix A.2.

For a rectangular plate simply supported on two opposite sides, the acoustic pressure can be further simplified as

$$F_{\text{pres}}(x_0, y_0, z_0, t) = \frac{\rho_0 p_0}{2\pi r} \sum_{m=1}^{\infty} \sum_{n=1}^{\infty} \frac{Y_n(e_0)\lambda_m^2 \upsilon_x^2}{\tilde{m}_{mn}(\omega_{mn}^2 - \lambda_m^2 \upsilon_x^2)} \cdot \times \left\{ (d_{12}^{mn} d_{22}^{mn} - d_{11}^{mn} d_{21}^{mn}) \sin\left[\lambda_m \upsilon_x \left(t - \frac{r}{c}\right)\right] + (d_{11}^{mn} d_{22}^{mn} + d_{12}^{mn} d_{21}^{mn}) \cos\left[\lambda_m \upsilon_x \left(t - \frac{r}{c}\right)\right] - \frac{\omega_{mn}}{\lambda_m \upsilon_x} \left[(e_{12}^{mn} e_{22}^{mn} - e_{11}^{mn} e_{21}^{mn}) \sin\left[\omega_{mn}\left(t - \frac{r}{c}\right)\right] + (e_{11}^{mn} e_{22}^{mn} + e_{12}^{mn} e_{21}^{mn}) \cos\left[\omega_{mn}\left(t - \frac{r}{c}\right)\right]\right]\right\}, \tag{49}$$

where the parameters d_{ij}^{mn} and e_{ij}^{mn} $(i,j = 1,2)$ are given in Appendix A.3. For the special case of all the four sides being simply supported, Eq. (49) still applies but the parameters e_{11}^{mn}, e_{12}^{mn}, e_{21}^{mn} and e_{22}^{mn} take different forms as shown in Appendix A.3.

4. Numerical results and discussions

The properties of the rectangular orthotropic plate chosen for numerical study are length $a = 10.8\,\text{m}$, breadth $b = 3.6\,\text{m}$, thickness $h = 0.15\,\text{m}$, density $\rho = 2400\,\text{kg/m}^3$, Poisson's ratio $v_x = 0.3$ and flexural rigidity $D_x = 1.5 \times 10^5\,\text{kN m}^2$ in the x-direction, damping coefficient $c_d = 0$, and rigidity ratios $D_y/D_x = 0.5$ and $H/D_x = 0.5$. The properties of air as the acoustic medium are density $\rho_0 = 1.29\,\text{kg/m}^3$ and speed of sound $c = 340\,\text{m/s}$. The observation point is 2 m above the centre of the plate, namely at (5.4 m, 1.8 m, 2.0 m). Unless otherwise specified, the plate in the standard case is simply supported at $x = 0$ and $x = a$ with the two other sides free. A moving load of constant magnitude $p_0 = 4.5\,\text{kN}$ moves at a constant speed $\upsilon_x = 20\,\text{m/s}$ in the x-direction along the longitudinal centreline (i.e. $e = 0\,\text{m}$). The inertia effect of the moving load is ignored. The plate is assumed to be undamped. The number of terms used are $m_u = 8$ and $n_u = 8$. In all the cases, the time τ required for the moving load to go across the plate is divided into 100 time steps.

4.1. Rectangular plate simply supported on two sides under a light moving load

The force $p_0 = 4.5\,\text{kN}$ moves at a constant speed $\upsilon_x = 20\,\text{m/s}$ in the x-direction at a variable distance e_0 from the x-axis. Fig. 3 shows the variations of the sound pressure at the observation point P with the eccentricity $e = b/2 - e_0$ with respect to the longitudinal centreline. It is seen that the larger the eccentricity e, the smaller the sound pressure received from the plate.

Then the effect of speed is next investigated. The moving force $p_0 = 4.5\,\text{kN}$ is to travel along the longitudinal centreline (i.e. $e = 0\,\text{m}$) at three different speeds $\upsilon_x = 10, 20$ and $30\,\text{m/s}$. The variations of the sound pressure at the observation point P are plotted against the time ratio t/τ in Fig. 4. It is observed that the higher the speed, the larger the sound pressure generated.

To investigate the effect of the damping coefficient, three cases are studied, i.e. $c_d = 0$, 1080 and 2160. The moving force $p_0 = 4.5\,\text{kN}$ is to travel along the longitudinal centreline (i.e. $e = 0\,\text{m}$) at speed $\upsilon_x = 20\,\text{m/s}$. Fig. 5 shows the effect of damping on the sound pressure generated. In general, it is seen that the larger the damping coefficient, the smaller the sound pressure. Initially, the effect

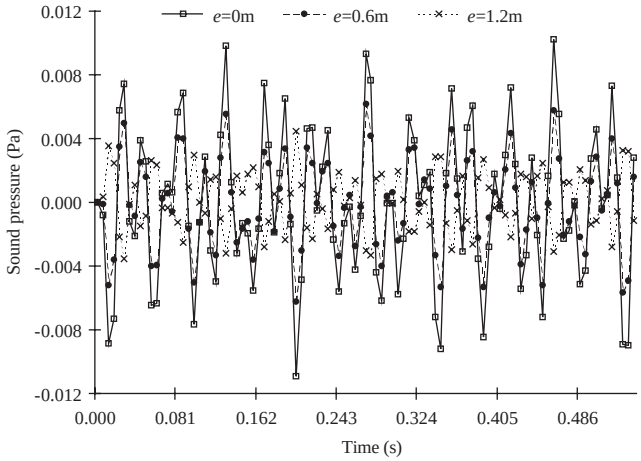

Fig. 3. Variation of sound pressure with eccentricity of path of moving load.

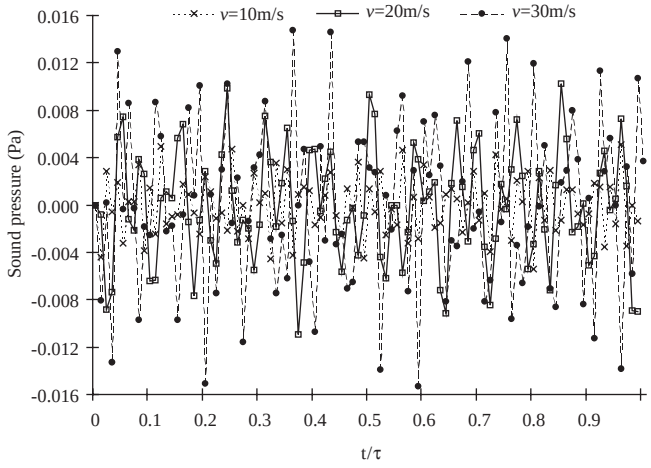

Fig. 4. Variation of sound pressure with the speed of moving load.

of damping is small. With the passage of time, the influence of damping is felt. The plate with higher damping tends to be less noisy in the long run.

4.2. Rectangular plate simply supported on two sides under moving load with inertia effect considered

In the previous cases, the inertia effect of the moving load has not been considered. To evaluate this effect, the case of a moving force $p_0 = 4.5\,\mathrm{kN}$ travelling along the longitudinal centreline (i.e. $e = 0\,\mathrm{m}$) at speed $v_x = 20\,\mathrm{m/s}$ is revisited. Fig. 6 shows the results considering and ignoring the inertia effect of the moving load. It is discovered that the sound pressure considering the mass

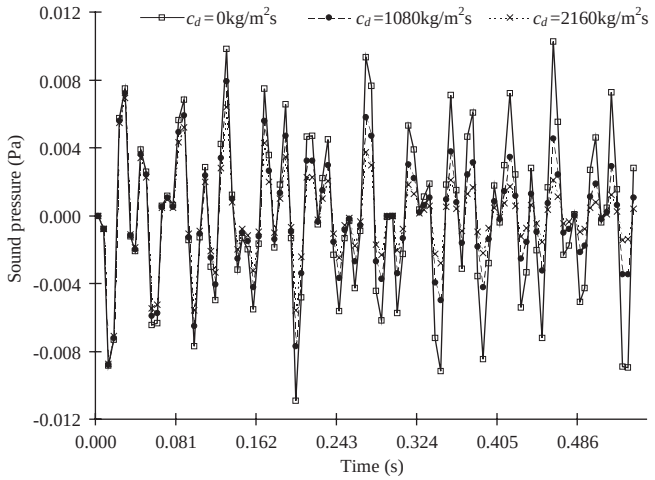

Fig. 5. Variation of sound pressure with damping.

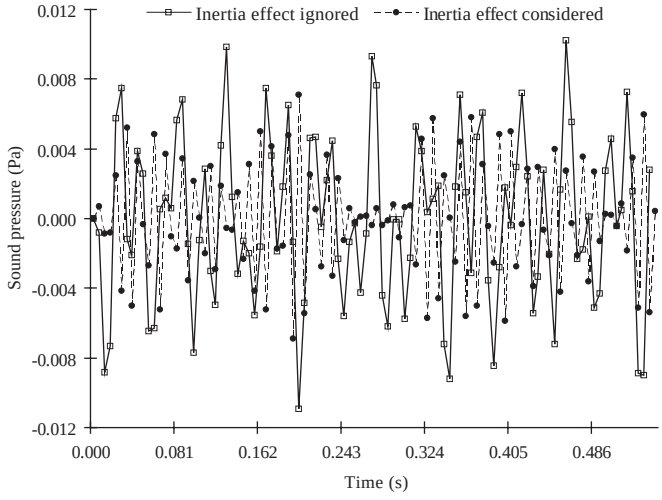

Fig. 6. Effect of inertia of moving load.

effect is smaller than that neglecting it. Since the mass ratio between the moving load and the plate is 0.0386, the mass effect on sound pressure cannot be neglected. These results are consistent with the findings of Humar and Kashif [6].

5. Rectangular plate simply supported on four sides under light moving load

The standard case is re-analysed with the plate simply supported on four sides. Fig. 7 compares the sound pressure generated against that in the standard case. In fact, these results reflect the effects of structural frequency distribution and loading frequency content. It is seen that the larger

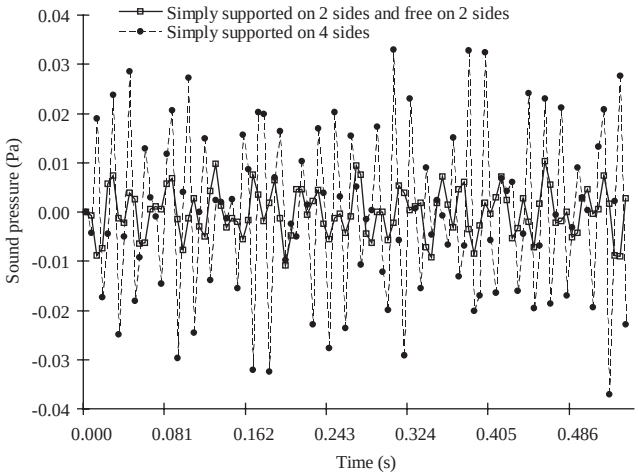

Fig. 7. Effect of boundary conditions.

the global stiffness of plate, the higher the structural frequencies, and the larger the sound pressure caused by moving loads. Therefore, the boundary conditions do affect the sound pressure generated by moving loads.

6. Conclusions

The vibrations of a rectangular orthotropic thin plate with general boundary conditions traversed by moving loads are first solved analytically. The effects of light and heavy moving loads are separately studied. Based on the Rayleigh integral and the analytical dynamic response of the plate, the acoustic pressure distributions around the plate are obtained in the time domain. Simplified methods for calculation of the acoustic pressure distributions in far field are developed. Numerical simulations have been carried out to investigate the effects of moving mass, damping coefficient, boundary conditions and moving speed on the dynamic responses of the plate and the acoustic pressure distributions. It confirms that the sound pressure drops with the distance from the path of moving load. It is observed that the higher the speed, the larger the sound pressure generated. Damping is normally effective in reducing the sound pressure generated. The inertia effect of the moving load tends to reduce the sound pressure, and therefore the mass of heavy moving loads should be considered. The boundary conditions do affect the acoustic pressure generated by moving loads. It is seen that the stiffer the plate, the higher the structural frequencies, and the larger the sound pressure caused by moving loads.

Acknowledgement

The work described in this paper has been supported by the Committee on Research and Conference Grants, The University of Hong Kong, China.

A. Appendix

A.1. Rectangular plates under heavy moving loads

For rectangular plates under heavy moving loads as discussed in Section 2.3, the equation of motion with the m- and n-series truncated after m_u and n_u terms, respectively, appears as

$$([I]+[M_m])\{\ddot{Q}\}+([C_d]+[C_m])\{\dot{Q}\}+([K_d]+[K_m])\{Q\}=\{P\}, \quad (41)$$

where

$$\{Q\}=[q_{11}\cdots q_{1n_u}\cdots q_{m_u1}\cdots q_{m_un_u}]^{\mathrm{T}}, \quad (42)$$

$$[M_m]=\mu_p\begin{bmatrix} \frac{U_{11}^2}{\tilde{m}_{11}} & \cdots & \frac{U_{11}U_{1n_u}}{\tilde{m}_{11}} & \cdots & \frac{U_{11}U_{m_u1}}{\tilde{m}_{11}} & \cdots & \frac{U_{11}U_{m_un_u}}{\tilde{m}_{11}} \\ \cdots & \cdots & \cdots & \cdots & \cdots & \cdots & \cdots \\ \frac{U_{1n_u}U_{11}}{\tilde{m}_{1n_u}} & \cdots & \frac{U_{1n_u}^2}{\tilde{m}_{1n_u}} & \cdots & \frac{U_{1n_u}U_{m_u1}}{\tilde{m}_{1n_u}} & \cdots & \frac{U_{1n_u}U_{m_un_u}}{\tilde{m}_{1n_u}} \\ \cdots & \cdots & \cdots & \cdots & \cdots & \cdots & \cdots \\ \frac{U_{m_u1}U_{11}}{\tilde{m}_{m_u1}} & \cdots & \frac{U_{m_u1}U_{1n_u}}{\tilde{m}_{m_u1}} & \cdots & \frac{U_{m_u1}^2}{\tilde{m}_{m_u1}} & \cdots & \frac{U_{m_u1}U_{m_un_u}}{\tilde{m}_{m_u1}} \\ \cdots & \cdots & \cdots & \cdots & \cdots & \cdots & \cdots \\ \frac{U_{m_un_u}U_{11}}{\tilde{m}_{m_un_u}} & \cdots & \frac{U_{m_un_u}U_{1n_u}}{\tilde{m}_{m_un_u}} & \cdots & \frac{U_{m_un_u}U_{m_u1}}{\tilde{m}_{m_un_u}} & \cdots & \frac{U_{m_un_u}^2}{\tilde{m}_{m_un_u}} \end{bmatrix}, \quad (A.1)$$

$$[C_d]=2\mathrm{Diag}(\zeta_{11}\omega_{11}\cdots\zeta_{1n_u}\omega_{1n_u}\zeta_{21}\omega_{21}\cdots\zeta_{2n_u}\omega_{2n_u}\zeta_{m_u1}\omega_{m_u1}\cdots\zeta_{m_un_u}\omega_{m_un_u}), \quad (A.2)$$

$$[C_m]=2v_x\mu_p\begin{bmatrix} \frac{U_{11}U'_{11}}{\tilde{m}_{11}} & \cdots & \frac{U_{11}U'_{1n_u}}{\tilde{m}_{11}} & \cdots & \frac{U_{11}U'_{m_u1}}{\tilde{m}_{11}} & \cdots & \frac{U_{11}U'_{m_un_u}}{\tilde{m}_{11}} \\ \cdots & \cdots & \cdots & \cdots & \cdots & \cdots & \cdots \\ \frac{U_{1n_u}U'_{11}}{\tilde{m}_{1n_u}} & \cdots & \frac{U_{1n_u}U'_{1n_u}}{\tilde{m}_{1n_u}} & \cdots & \frac{U_{1n_u}U'_{m_u1}}{\tilde{m}_{1n_u}} & \cdots & \frac{U_{1n_u}U'_{m_un_u}}{\tilde{m}_{1n_u}} \\ \cdots & \cdots & \cdots & \cdots & \cdots & \cdots & \cdots \\ \frac{U_{m_u1}U'_{11}}{\tilde{m}_{m_u1}} & \cdots & \frac{U_{m_u1}U'_{1n_u}}{\tilde{m}_{m_u1}} & \cdots & \frac{U_{m_u1}U'_{m_u1}}{\tilde{m}_{m_u1}} & \cdots & \frac{U_{m_u1}U'_{m_un_u}}{\tilde{m}_{m_u1}} \\ \cdots & \cdots & \cdots & \cdots & \cdots & \cdots & \cdots \\ \frac{U_{m_un_u}U'_{11}}{\tilde{m}_{m_un_u}} & \cdots & \frac{U_{m_un_u}U'_{1n_u}}{\tilde{m}_{m_un_u}} & \cdots & \frac{U_{m_un_u}U'_{m_u1}}{\tilde{m}_{m_un_u}} & \cdots & \frac{U_{m_un_u}U'_{m_un_u}}{\tilde{m}_{m_un_u}} \end{bmatrix}, \quad (A.3)$$

$$[K_d]=\mathrm{Diag}(\omega_{11}^2\cdots\omega_{1n_u}^2 \quad \omega_{21}^2\cdots\omega_{2n_u}^2 \quad \omega_{m_u1}^2\cdots\omega_{m_un_u}^2), \quad (A.4)$$

$$[K_m] = \mu_p v_x^2 \begin{bmatrix} \frac{U_{11}U''_{11}}{\tilde{m}_{11}} & \cdots & \frac{U_{11}U''_{1n_u}}{\tilde{m}_{11}} & \cdots & \frac{U_{11}U''_{m_u1}}{\tilde{m}_{11}} & \cdots & \frac{U_{11}U''_{m_un_u}}{\tilde{m}_{11}} \\ \cdots & \cdots & \cdots & \cdots & \cdots & \cdots & \cdots \\ \frac{U_{1n_u}U''_{11}}{\tilde{m}_{1n_u}} & \cdots & \frac{U_{1n_u}U''_{1n_u}}{\tilde{m}_{1n_u}} & \cdots & \frac{U_{1n_u}U''_{m_u1}}{\tilde{m}_{1n_u}} & \cdots & \frac{U_{1n_u}U''_{m_un_u}}{\tilde{m}_{1n_u}} \\ \cdots & \cdots & \cdots & \cdots & \cdots & \cdots & \cdots \\ \frac{U_{m_u1}U''_{11}}{\tilde{m}_{m_u1}} & \cdots & \frac{U_{m_u1}U''_{1n_u}}{\tilde{m}_{m_u1}} & \cdots & \frac{U_{m_u1}U''_{m_u1}}{\tilde{m}_{m_u1}} & \cdots & \frac{U_{m_u1}U''_{m_un_u}}{\tilde{m}_{m_u1}} \\ \cdots & \cdots & \cdots & \cdots & \cdots & \cdots & \cdots \\ \frac{U_{m_un_u}U''_{11}}{\tilde{m}_{m_un_u}} & \cdots & \frac{U_{m_un_u}U''_{1n_u}}{\tilde{m}_{m_un_u}} & \cdots & \frac{U_{m_un_u}U''_{m_u1}}{\tilde{m}_{m_un_u}} & \cdots & \frac{U_{m_un_u}U''_{m_un_u}}{\tilde{m}_{m_un_u}} \end{bmatrix}, \tag{A.5}$$

$$\{P\} = [p_{11} \cdots p_{1n_u} \quad p_{21} \cdots p_{2n_u} \quad p_{m_u1} \cdots p_{m_un_u}]^{\mathrm{T}}, \tag{A.6}$$

$$U_{ij} = U_{ij}(v_x t, e_0), \quad U'_{ij} = \left.\frac{\partial U_{ij}}{\partial x}\right|_{\substack{x=v_x t \\ y=e_0}}, \quad U''_{ij} = \left.\frac{\partial^2 U_{ij}}{\partial x^2}\right|_{\substack{x=v_x t \\ y=e_0}}. \tag{A.7}$$

A.2. Far-field acoustic pressure distribution of plates with general boundary conditions under light moving load

The far-field acoustic pressure distribution of plates with general boundary conditions and negligible damping under light moving load is given by

$$\begin{aligned} F_{\mathrm{pres}}(x_0, y_0, z_0, t) = \frac{\rho_0 p_0}{2\pi r} \sum_{m=1}^{\infty} \sum_{n=1}^{\infty} \frac{Y_n(e_0)}{\tilde{m}_{mn}} \{ & \Delta_{1mn}(a_{12}^{mn} a_{22}^{mn} - a_{11}^{mn} a_{21}^{mn}) + \Delta_{2mn}(a_{11}^{mn} a_{22}^{mn} + a_{12}^{mn} a_{21}^{mn}) \\ & + \Delta_{3mn}(b_{12}^{mn} b_{22}^{mn} - b_{11}^{mn} b_{21}^{mn}) + \Delta_{4mn}(b_{11}^{mn} b_{22}^{mn} + b_{12}^{mn} b_{21}^{mn}) + \Delta_{5mn}(c_{12}^{mn} c_{22}^{mn} + c_{11}^{mn} c_{21}^{mn}) \\ & + \Delta_{6mn}(c_{11}^{mn} c_{22}^{mn} + c_{12}^{mn} c_{21}^{mn})\}, \end{aligned} \tag{48}$$

where

$$\Delta_{1mn} = -\omega_{mn}^2 \left[E'_{mn} \sin \omega_{mn}\left(t - \frac{r}{c}\right) + F'_{mn} \cos \omega_{mn}\left(t - \frac{r}{c}\right)\right], \tag{A.8}$$

$$\Delta_{2mn} = -\omega_{mn}^2 \left[E'_{mn} \cos \omega_{mn}\left(t - \frac{r}{c}\right) - F'_{mn} \sin \omega_{mn}\left(t - \frac{r}{c}\right)\right], \tag{A.9}$$

$$\Delta_{3mn} = -\alpha_m^2 v_x^2 \left[G'_{mn} \sin \alpha_m v_x \left(t - \frac{r}{c}\right) + H'_{mn} \cos \alpha_m v_x \left(t - \frac{r}{c}\right)\right], \tag{A.10}$$

$$\Delta_{4mn} = -\alpha_m^2 v_x^2 \left[G'_{mn} \cos \alpha_m v_x \left(t - \frac{r}{c}\right) - H'_{mn} \sin \alpha_m v_x \left(t - \frac{r}{c}\right)\right], \tag{A.11}$$

$$\Delta_{5mn} = \alpha_m^2 v_x^2 \left[I'_{mn} \operatorname{sh} \alpha_m v_x \left(t - \frac{r}{c}\right) + J'_{mn} \operatorname{ch} \alpha_m v_x \left(t - \frac{r}{c}\right)\right], \tag{A.12}$$

$$\Delta_{6mn} = \alpha_m^2 v_x^2 \left[I'_{mn} \operatorname{ch} \alpha_m v_x \left(t - \frac{r}{c}\right) + J'_{mn} \operatorname{sh} \alpha_m v_x \left(t - \frac{r}{c}\right)\right], \tag{A.13}$$

$$a_{11}^{mn} = \int_0^a X_m(x) \sin\left(\frac{\omega_{mn}}{c}\frac{x_0}{r}x\right) \mathrm{d}x = \int_0^a X_m(x) \sin\left(\frac{\omega_{mn}}{c}x \sin\theta \cos\phi\right) \mathrm{d}x, \tag{A.14}$$

$$a_{12}^{mn} = \int_0^a X_m(x) \cos\left(\frac{\omega_{mn}}{c}\frac{x_0}{r}x\right) \mathrm{d}x = \int_0^a X_m(x) \cos\left(\frac{\omega_{mn}}{c}x \sin\theta \cos\phi\right) \mathrm{d}x, \tag{A.15}$$

$$a_{21}^{mn} = \int_0^b Y_n(y) \sin\left(\frac{\omega_{mn}}{c}\frac{y_0}{r}y\right) \mathrm{d}y = \int_0^b Y_n(y) \sin\left(\frac{\omega_{mn}}{c}y \sin\theta \sin\phi\right) \mathrm{d}y, \tag{A.16}$$

$$a_{22}^{mn} = \int_0^b Y_n(y) \cos\left(\frac{\omega_{mn}}{c}\frac{y_0}{r}y\right) \mathrm{d}y = \int_0^b Y_n(y) \cos\left(\frac{\omega_{mn}}{c}y \sin\theta \sin\phi\right) \mathrm{d}y, \tag{A.17}$$

$$b_{11}^{mn} = \int_0^a X_m(x) \sin\left(\frac{\alpha_m \upsilon_x}{c}\frac{x_0}{r}x\right) \mathrm{d}x = \int_0^a X_m(x) \sin\left(\frac{\alpha_m \upsilon_x}{c}x \sin\theta \cos\phi\right) \mathrm{d}x, \tag{A.18}$$

$$b_{12}^{mn} = \int_0^a X_m(x) \cos\left(\frac{\alpha_m \upsilon_x}{c}\frac{x_0}{r}x\right) \mathrm{d}x = \int_0^a X_m(x) \cos\left(\frac{\alpha_m \upsilon_x}{c}x \sin\theta \cos\phi\right) \mathrm{d}x, \tag{A.19}$$

$$b_{21}^{mn} = \int_0^b Y_n(y) \sin\left(\frac{\alpha_m \upsilon_x}{c}\frac{y_0}{r}y\right) \mathrm{d}y = \int_0^b Y_n(y) \sin\left(\frac{\alpha_m \upsilon_x}{c}y \sin\theta \sin\phi\right) \mathrm{d}y, \tag{A.20}$$

$$b_{22}^{mn} = \int_0^b Y_n(y) \cos\left(\frac{\alpha_m \upsilon_x}{c}\frac{y_0}{r}y\right) \mathrm{d}y = \int_0^b Y_n(y) \cos\left(\frac{\alpha_m \upsilon_x}{c}y \sin\theta \sin\phi\right) \mathrm{d}y, \tag{A.21}$$

$$c_{11}^{mn} = \int_0^a X_m(x) \operatorname{sh}\left(\frac{\alpha_m \upsilon_x}{c}\frac{x_0}{r}x\right) \mathrm{d}x = \int_0^a X_m(x) \operatorname{sh}\left(\frac{\alpha_m \upsilon_x}{c}x \sin\theta \cos\phi\right) \mathrm{d}x, \tag{A.22}$$

$$c_{12}^{mn} = \int_0^a X_m(x) \operatorname{ch}\left(\frac{\alpha_m \upsilon_x}{c}\frac{x_0}{r}x\right) \mathrm{d}x = \int_0^a X_m(x) \operatorname{ch}\left(\frac{\alpha_m \upsilon_x}{c}x \sin\theta \cos\phi\right) \mathrm{d}x, \tag{A.23}$$

$$c_{21}^{mn} = \int_0^b Y_n(y) \operatorname{sh}\left(\frac{\alpha_m \upsilon_x}{c}\frac{y_0}{r}y\right) \mathrm{d}y = \int_0^b Y_n(y) \operatorname{sh}\left(\frac{\alpha_m \upsilon_x}{c}y \sin\theta \sin\phi\right) \mathrm{d}y, \tag{A.24}$$

$$c_{22}^{mn} = \int_0^b Y_n(y) \operatorname{ch}\left(\frac{\alpha_m \upsilon_x}{c}\frac{y_0}{r}y\right) \mathrm{d}y = \int_0^b Y_n(y) \operatorname{ch}\left(\frac{\alpha_m \upsilon_x}{c}y \sin\theta \sin\phi\right) \mathrm{d}y, \tag{A.25}$$

A.3. Far-field acoustic pressure distribution of plates simply supported on two opposite sides under light moving load

The far-field acoustic pressure distribution of plates simply supported on two opposite sides with negligible damping under light moving load is given by

$$F_{\text{pres}}(x_0, y_0, z_0, t) = \frac{\rho_0 p_0}{2\pi r} \sum_{m=1}^{\infty} \sum_{n=1}^{\infty} \frac{Y_n(e_0)\lambda_m^2 \upsilon_x^2}{\tilde{m}_{mn}(\omega_{mn}^2 - \lambda_m^2 \upsilon_x^2)} \times \left\{ (d_{12}^{mn} d_{22}^{mn} - d_{11}^{mn} d_{21}^{mn}) \sin\left[\lambda_m \upsilon_x \left(t - \frac{r}{c}\right)\right] + (d_{11}^{mn} d_{22}^{mn} + d_{12}^{mn} d_{21}^{mn}) \cos\left[\lambda_m \upsilon_x \left(t - \frac{r}{c}\right)\right] - \frac{\omega_{mn}}{\lambda_m \upsilon_x} \left[(e_{12}^{mn} e_{22}^{mn} - e_{11}^{mn} e_{21}^{mn}) \sin\left[\omega_{mn}\left(t - \frac{r}{c}\right)\right] + (e_{11}^{mn} e_{22}^{mn} + e_{12}^{mn} e_{21}^{mn}) \cos\left[\omega_{mn}\left(t - \frac{r}{c}\right)\right]\right] \right\}, \tag{49}$$

where

$$d_{11}^{mn} = -\frac{(-1)^m \lambda_m \sin((\lambda_m \upsilon_x/c)(x_0/r)a)}{\lambda_m^2 - (\lambda_m \upsilon_x/c)^2 (x_0/r)^2} = -\frac{(-1)^m \lambda_m \sin((\lambda_m \upsilon_x/c)a \sin\theta \cos\phi)}{\lambda_m^2 - (\lambda_m \upsilon_x/c)^2 (\sin\theta \cos\phi)^2}, \tag{A.26}$$

$$d_{12}^{mn} = -\frac{\lambda_m[(-1)^m \cos((\lambda_m \upsilon_x/c)(x_0/r)a) - 1]}{\lambda_m^2 - (\lambda_m \upsilon_x/c)^2 (x_0/r)^2} = -\frac{\lambda_m[(-1)^m \cos((\lambda_m \upsilon_x/c)a \sin\theta \cos\phi) - 1]}{\lambda_m^2 - (\lambda_m \upsilon_x/c)^2 (\sin\theta \cos\phi)^2}, \tag{A.27}$$

$$d_{21}^{mn} = \int_0^b Y_n(y) \sin\left(\frac{\lambda_m \upsilon_x}{c} \frac{y_0}{r} y\right) \mathrm{d}y = \int_0^b Y_n(y) \sin\left(\frac{\lambda_m \upsilon_x}{c} y \sin\theta \sin\phi\right) \mathrm{d}y, \tag{A.28}$$

$$d_{22}^{mn} = \int_0^b Y_n(y) \cos\left(\frac{\lambda_m \upsilon_x}{c} \frac{y_0}{r} y\right) \mathrm{d}y = \int_0^b Y_n(y) \cos\left(\frac{\lambda_m \upsilon_x}{c} y \sin\theta \sin\phi\right) \mathrm{d}y, \tag{A.29}$$

$$e_{11}^{mn} = -\frac{(-1)^m \lambda_m \sin((\omega_{mn}/c)(x_0/r)a)}{\lambda_m^2 - (\omega_{mn}/c)^2 (x_0/r)^2} = -\frac{(-1)^m \lambda_m \sin((\omega_{mn}/c)a \sin\theta \cos\phi)}{\lambda_m^2 - (\omega_{mn}/c)^2 (\sin\theta \cos\phi)^2}, \tag{A.30}$$

$$e_{12}^{mn} = -\frac{\lambda_m[(-1)^m \cos((\omega_{mn}/c)(x_0/r)a) - 1]}{\lambda_m^2 - (\omega_{mn}/c)^2 (x_0/r)^2} = -\frac{\lambda_m[(-1)^m \cos((\omega_{mn}/c)a \sin\theta \cos\phi) - 1]}{\lambda_m^2 - (\omega_{mn}/c)^2 (\sin\theta \cos\phi)^2}, \tag{A.31}$$

$$e_{21}^{mn} = \int_0^b Y_n(y) \sin\left(\frac{\omega_{mn}}{c} \frac{y_0}{r} y\right) \mathrm{d}y = \int_0^b Y_n(y) \sin\left(\frac{\omega_{mn}}{c} y \sin\theta \sin\phi\right) \mathrm{d}y, \tag{A.32}$$

$$e_{22}^{mn} = \int_0^b Y_n(y) \cos\left(\frac{\omega_{mn}}{c} \frac{y_0}{r} y\right) \mathrm{d}y = \int_0^b Y_n(y) \cos\left(\frac{\omega_{mn}}{c} y \sin\theta \sin\phi\right) \mathrm{d}y, \tag{A.33}$$

For the special case of all four sides being simply supported, Eq. (49) still applies but the parameters e_{11}^{mn}, e_{12}^{mn}, e_{21}^{mn} and e_{22}^{mn} take different forms as follows:

$$e_{11}^{mn} = -\frac{(-1)^n \mu_n \sin((\lambda_m v_x/c)(y_0/r)b)}{\mu_n^2 - (\lambda_m v_x/c)^2 (y_0/r)^2} = -\frac{(-1)^n \mu_n \sin((\lambda_m v_x/c)b \sin\theta \sin\phi)}{\mu_n^2 - (\lambda_m v_x/c)^2 (\sin\theta \sin\phi)^2}, \tag{A.34}$$

$$e_{12}^{mn} = -\frac{\mu_n[(-1)^n \cos((\lambda_m v_x/c)(y_0/r)b) - 1]}{\mu_n^2 - (\lambda_m v_x/c)^2 (y_0/r)^2} = -\frac{\mu_n[(-1)^n \cos((\lambda_m v_x/c)b \sin\theta \sin\phi) - 1]}{\mu_n^2 - (\lambda_m v_x/c)^2 (\sin\theta \sin\phi)^2}, \tag{A.35}$$

$$e_{21}^{mn} = -\frac{(-1)^n \mu_n \sin((\omega_{mn}/c)(y_0/r)b)}{\mu_n^2 - (\omega_{mn}/)c^2 (y_0/r)^2} = -\frac{(-1)^n \mu_n \sin((\omega_{mn}/c)b \sin\theta \sin\phi)}{\mu_n^2 - (\omega_{mn}/c)^2 (\sin\theta \sin\phi)^2}, \tag{A.36}$$

$$e_{22}^{mn} = -\frac{\mu_n[(-1)^n \cos((\omega_{mn}/c)(y_0/r)b) - 1]}{\mu_n^2 - (\omega_{mn}/c)^2 (y_0/r)^2} = -\frac{\mu_n[(-1)^n \cos((\omega_{mn}/c)b \sin\theta \sin\phi) - 1]}{\mu_n^2 - (\omega_{mn}/c)^2 (\sin\theta \sin\phi)^2}. \tag{A.37}$$

References

[1] T.F. Raske, A.L. Schlack Jr., Dynamic response of plates due to moving loads, *Journal of the Acoustical Society of America* 42 (3) (1967) 625–635.

[2] L. Fryba, *Vibration of Solids and Structures under Moving Loads*, Thomas Telford, London, UK, 1999.

[3] D.M. Yoshida, W. Weaver, Finite element analysis of beams and plates with moving loads, *Publications, International Association of Bridges and Structural Engineering* 31 (1) (1971) 79–195.

[4] J.S. Wu, M.L. Lee, T.S. Lai, The dynamic analysis of a flat plate under a moving load by the finite element method, *International Journal for Numerical Methods in Engineering* 193 (1) (1996) 307–314.

[5] J.A. Gbadeyan, S.T. Oni, Dynamic behavior of beams and rectangular plates under moving loads, *Journal of Sound and Vibration* 182 (5) (1995) 677–695.

[6] J.L. Humar, A.H. Kashif, Dynamic response analysis of slab-type bridges, *Journal of Structural Engineering* 121 (1) (1995) 48–62.

[7] H. Takabatake, Dynamic analysis of rectangular plates with stepped thickness subjected to moving loads including additional mass, *Journal of Sound and Vibration* 213 (5) (1998) 829–842.

[8] R.T. Wang, N.Y. Kuo, Nonlinear vibration of Mindlin plate subjected to moving forces including the effect of weight of the plate, *Structural Engineering and Mechanics* 8 (2) (1999) 151–164.

[9] Y.K. Cheung, F.T.K. Au, D.Y. Zheng, Y.S. Cheng, Vibration of bridges under moving vehicles by structural impedance method (SIM) and finite strip method (FSM), in: *Proceedings of the 13th ASCE Engineering Mechanics Division Conference*, Baltimore, MD, June 13–16, 1999, p. 6.

[10] M.R. Shadnam, M. Mofid, J.E. Akin, On the dynamic response of rectangular plate with moving mass, *Thin-Walled Structures* 39 (9) (2001) 797–806.

[11] G. Maidanik, Response of ribbed panels, *Journal of the Acoustical Society of America* 34 (1962) 809–835.

[12] C.E. Wallace, Radiation resistance of rectangular panels, *Journal of the Acoustical Society of America* 53 (1972) 946–952.

[13] G. Maidanik, Vibrational and radiative classification of modes of a baffled finite panel, *Journal of Sound and Vibration* 34 (1974) 447–455.

[14] E.G. Williams, J.D. Maynard, Numerical evaluation of the Rayleigh integral for planar radiators using the FFT, *Journal of the Acoustical Society of America* 72 (6) (1982) 2020–2030.

[15] S. Schedin, C. Lambourge, A. Chaigne, Transient sound fields from impacted plates: comparison between numerical simulations and experiments, *Journal of Sound and Vibration* 221 (3) (1999) 471–490.
[16] F.J. Fahy, *Sound and Structural Vibration: Radiation, Transmission and Response*, Academic Press, London, 1985.
[17] L. Cremer, M. Heckl, E.E. Ungar, *Structure-Borne Sound*, Springer, Berlin, 1988.
[18] N.J.Jr. Huffington, W.H. Hoppmann II, On the transverse vibrations of rectangular orthotropic plates, *Journal of Applied Mechanics* 25 (3) (1958) 389–395.
[19] A.W. Leissa, *Vibration of Plates, NASA SP-160*, NASA, Washington, DC, 1969.
[20] M.F. Wang, F.T.K. Au, Higher-order schemes for time integration in dynamic structural analysis, *Journal of Sound and Vibration* 278 (3) (2004) 690–698.